Inversion of time domain IP data from inductive sources

Douglas W. Oldenburg, Seogi Kang, and David Marchant*
Geophysical Inversion Facility, University of British Columbia, Canada

Summary

The recovery of chargeability information from inductive sources is treated as a workflow process with the following steps: (a) invert early time, non-IP-contaminated, responses to obtain a background conductivity; (b) compute raw d^{IP} data by subtracting the forward modelled TEM responses from the observations; (c) process (possibly) the raw d^{IP} data; (d) generate a linear sensitivity function that relates the IP data to a pseudo-chargeability; (e) carry out a 3D inversion to recover the pseudo-chargeability for that time channel; (f) perform an inversion at multiple time channels, either independently or simultaneously. In any workflow sequence, a poorly executed step can generate erroneous results. In this paper we investigate the workflow elements and identify their importance and robustness in the inversion process. To achieve this we build a synthetic model composed of a number of chargeable and conductive bodies buried in a variable conductive background. We show that our strategy has much potential for making inferences about existence, geometry and relative strength of chargeable bodies. The methodology is applied to two field examples.

Introduction

The electrical conductivity of earth materials can be frequency dependent due to the build-up of charges that occur under the application of an electric field. Effectively, the rock is electrically polarized. Polarization charges can accumulate whenever there is an electric field in a medium and so the transmitter can be a galvanic or inductive source. Here we restrict attention to inductive sources and, in particular, focus upon airborne systems such as the coincident loop (VTEM) instrument which measures db_z/dt data. These data are often observed to have negative transients for late time channels. Weidelt (1982) showed that the most plausible explanation of these is that they are caused by IP effects.

To extract chargeability information from inductive sources we use ideas that have been fruitful in the analysis of ground EIP where the IP phenomenon generates a perturbation to the electrical conductivity (Seigel, 1959). This allows us to set up a linear inverse problem to recover a pseudo-chargeability. The primary difference between inductive source IP and traditional EIP is that the electric fields in the earth never achieve a steady-state but rather they continually change in time. Thus a region in the earth charges and discharges in a complex manner and the polarization current at any time is the convolution of the conductivity response function with the existing electric field. Any pseudo-chargeability must incorporate these dynamics. Because of this time history, polarization currents from an inductive source are smaller than those achieved with an EIP survey and its steady state electric field. It follows that we are still dealing with small perturbations, and hence the same linearization techniques, that have served so well for EIP, should also be applicable for inductive sources. That has been a motivation for development of our procedure. In the following we first provide some mathematical background, introduce our synthetic model, and step through the workflow process.

Decomposition of IP responses

A commonly-used expression to model complex conductivity in the frequency domain is the Cole-Cole model (Cole and Cole, 1941):

$$\sigma(\omega) = \sigma_\infty - \sigma_\infty \frac{\eta}{1+(1-\eta)(\imath\omega\tau)^c}, \tag{1}$$

where σ_∞ is the conductivity at infinite frequency, ω is the angular frequency, η is the intrinsic chargeability, τ is the time constant and c is the frequency dependency. By applying the inverse Fourier transform we have

$$\sigma(t) = \mathscr{F}^{-1}[\sigma(\omega)] = \sigma_\infty \delta(t) + \triangle\sigma(t) \tag{2}$$

where $\delta(t)$ is the Dirac delta function and $\mathscr{F}^{-1}[\cdot]$ is the inverse Fourier transform operator. $\triangle\sigma(t)$ is often referred to as the response function. Consider Maxwell's equations in time domain:

$$\vec{\nabla} \times \frac{1}{\mu}\vec{b} - \vec{j} = \vec{j}_s, \tag{3}$$

$$\vec{\nabla} \times \vec{e} = -\frac{\partial \vec{b}}{\partial t}, \tag{4}$$

where $\vec{e}$ is the electric field (V/m), $\vec{b}$ is the magnetic flux density (T) and μ is the magnetic permeability (H/m). Here $\vec{j}$ is the conduction current. In the frequency domain the current density $\vec{J}$ is related to conductivity via $\vec{J}(\omega) = \sigma(\omega)\vec{E}(\omega)$. Converting this relationship to the time domain using the Fourier transform yields:

$$\vec{j}(t) = \sigma(t) \otimes \vec{e}(t), \tag{5}$$

where $\otimes$ stands for the convolution. That is, the current density depends upon the previous history of the electric field. As in Smith et al. (1988), we let $\vec{j} = \vec{j}^F + \vec{j}^{IP}$. Here superscripts F and IP respectively indicate EM responses

GEM Chengdu 2015: International Workshop on Gravity, Electrical & Magnetic Methods and Their Applications
Chengdu, China. April 19-22, 2015
*The corresponding author: doug@eos.ubc.ca.

without IP effects and to responses related only to polarization. With this decomposition, we write the fundamental and IP current densities as

$$\vec{j}^F(t) = \sigma_\infty \vec{e}^F(t), \tag{6}$$

$$\vec{j}^{IP} = \sigma_\infty \vec{e}^{IP}(t) + \triangle\sigma(t) \otimes \vec{e}(t). \tag{7}$$

Correspondingly, we decompose an EM response, *d,* into fundamental and IP parts; $d = d^F + d^{IP}$. By letting $F[\cdot]$ represent an operator associated with Maxwell's equations, we define the IP datum as

$$d^{IP} = d - d^F = F[\sigma_\infty \delta(t) + \triangle\sigma(t)] - F[\sigma_\infty \delta(t)] \tag{8}$$

This subtraction process acts as an EM decoupling process that reduces the EM effects to better recognize IP effects in the measured responses. This subtraction formed the basis of work by Routh and Oldenburg (2001). Thus, assuming we have a reasonable estimate for the distribution of σ_∞ in 3D space, we can identify the IP signal that is embedded in the measured responses.

3D synthetic model and survey

Geological environments have a range of conductive and resistive bodies, with different chargeability characteristics, buried in highly variable background conductivity. To encapsulate this variability we generate a synthetic model composed of 4 chargeable blocks that have different conductivity, chargeability, and depths of burial. The host medium has a variable conductivity. Plan and cross-section views are provided in Figure 1. An ATEM survey with 21 lines of data and 21 soundings per line is carried out using EMTDIP code (Marchant et al., 2015). A plot of the observed data at 1.25ms is shown on Figure 2(a). Block A3 shows a negative response but data over the other blocks are positive.

Recovering the background conductivity

Our IP data are defined by equation (8). To estimate σ_∞ we invert data at early time channels where IP effects are less than ambient noise. This is not a straight-forward matter but any sounding data that are negative should be discarded. The remaining data are inverted using standard Gauss-Newton inversion methodologies to recover a smoothed conductivity (Yang et al., 2014). The resultant conductivity is shown in Figure 3 and can be compared to the true conductivity in Figure 1.

The background conductivity plays two roles in our procedure. Through equation (8) it is used to define the d^{IP} data; it is also used to compute a linearized sensitivity function. We address the d^{IP} data first.

Generating d^{IP} data

The EM responses for our recovered model are shown in Figure 4 (b). Subtracting those from the observations produces the raw d^{IP} data in Figure 4(c). The result is a dramatic improvement. All four bodies now exhibit the negative responses expected for chargeable bodies. To examine this more closely we write

$$d^{IP}_{obs}(t) = d^{IP}_{true}(t) + \triangle d[\sigma_\infty](t) + n(t) \tag{9}$$

where $d^{IP}_{obs}(t)$ is raw d^{IP} data, $d^{IP}_{true}(t)$ are the true IP data, $\triangle d[\sigma_\infty](t)$ is the error caused because of a poor estimate of the background conductivity and *n(t)* is additive noise.

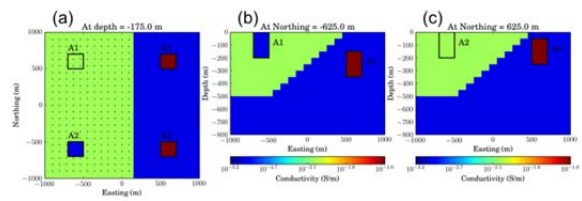

Figure 1: Plan and sections views of 3D σ_∞ model. Solid lines outline boundaries of four IP bodies.

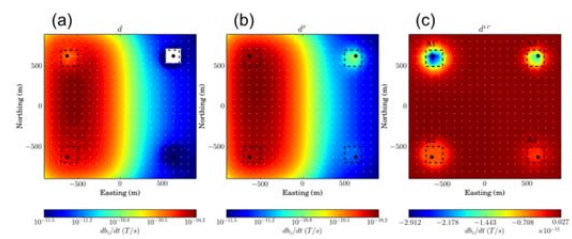

Figure 2: Responses at 1.25 ms. (a) Total, (b) fundamental and (c) true d^{IP} . A1-A4 indicate corresponding anomalies due to four IP bodies. Black dotted line contours boundaries of four IP bodies.

Undoubtedly there are situations where the errors on the right hand side can become larger than $d^{IP}_{true}(t)$. This will always occur at early time channels where the IP response is small and EM induction response is large. Thus there is an "earliest" time channel that can be used for this analysis. The second issue concerns $\triangle d[\sigma_\infty](t)$. This is more difficult to quantify and needs to be treated on a case-by-case basis. It is least important when dealing with resistive bodies and hosts and most problematic as the bodies and hosts become more conductive. There are a few items of note however. Firstly, if the background conductivity is incorrect by a scale factor then this shifts the d^{IP} data. Away from chargeable bodies the d^{IP} response should be zero. Assuming these locations can be recognized then the regional shift can be estimated and applied to the raw d^{IP} data. The same idea is applicable to long wavelength spatial components of $\triangle d[\sigma_\infty]$. Any corrective procedure, which is akin to removal of regional fields in potential fields processing, relies on identification of areas in the model believed to be free of IP responses. The procedure was

GEM Chengdu 2015: International Workshop on Gravity, Electrical & Magnetic Methods and Their Applications
Chengdu, China. April 19-22, 2015.

beneficial in a field data example for processing ATEM data at Mt. Milligan. It was not deemed necessary for the synthetic problem here and thus we will invert the data in Figure 4(c).

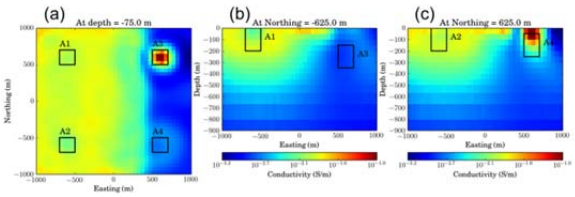

Figure 3: Plan and sections views of 3D σ_{est} model.

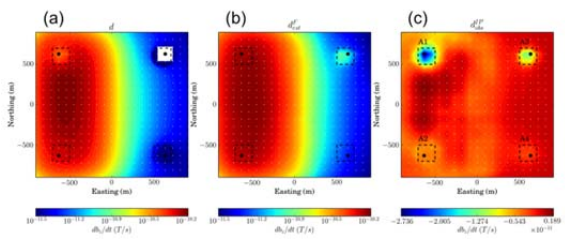

Figure 4: EM responses at 1.25ms. (a)Total, (b) estimated fundamental, and (c) raw d^{IP}. .

3D linearized inversion

There are two aspects of time domain inductive source IP that add complexity compared to regular EIP surveys. The first is the convolution term which relates the charge build up to the time history of the electric field. The second is that a steady state charging of the subsurface is never achieved. At any point in the earth, the electric field will increase and then decay as the induced fields from the source pass propagate through and decay. The IP signal of interest is usually at the times when the fundamental field has decayed. Nevertheless we choose a linearization approach that is similar to previous work done for EIP problems

The most important component of our linearization is the IP current density, $\vec{j}^{IP}$ and we first formulate a linear relationship between it and pseudo-chargeability. Once we have $\vec{j}^{IP}$, then $\vec{b}^{IP}$ or $\frac{\partial \vec{b}^{IP}}{\partial t}$ can be computed using Biot-Savart law and the TEM responses can be linearized as a function of pseudo-chargeability. Mathematical derivation of this linearization is clearly shown in Kang and Oldenburg (2015).

After this linearization, we can have a linear equation

$$\mathbf{d}^{IP}(t) = -\mathbf{J}\tilde{\eta}(t), \qquad (10)$$

where **J** is the sensitivity matrix. This is a linear relationship between the data and pseudo-chargeability. Here pseudo-chargeability is defined as

$$\tilde{\eta}(t) = -\frac{\triangle\sigma(t) \otimes w^e(t)}{\sigma_\infty} \qquad (11)$$

and the electric field is approximated as $\vec{e}(t) = \vec{e}^F_{max} w^e(t)$ where $\vec{e}^F_{max} = \vec{e}^F(t) \otimes \delta(t - t^{max})$ is the maximum fundamental electric field and $w^e(t)$ is a dimensionless function that prescribes the history of the electric field at each location. Following Oldenburg and Li (1994) we formulate the inverse problem and calculate a pseudo-chargeability distribution at each time channel. The pseudo-chargeability is a positive parameter and this provides an important constraint in the inverse problem. In addition, the d^{IP} data are potential field data and hence they have no inherent depth resolution. We therefore invert them as if they were static field magnetic data and incorporate a depth weighting ($\propto \frac{1}{r^3}$).

To illustrate our inversion procedure we perform a number of tests. First we compute d^{IP} data by equation (8) using the estimated conductivity model shown in Figure 3. The sensitivities are also generated with this approximate conductivity. The recovered chargeability model is shown in Figure 5(a). All four chargeable bodies are represented. This is encouraging since, in the original observations, there was no indication of negative values for three of the bodies (A1, A2, A4) at the time channel being investigated. To see the effect of using an approximate conductivity we carry out the same analysis but use the true conductivity to generate the d^{IP} data and the sensitivities. The recovered chargeability is shown in Figure 5(b).

The two inversions in Figures 5(a) and (b) are not identical but discrepancies are not major. The horizontal locations of the four chargeable bodies correspond well with the true model. Depth is not well constrained, but one should be cautious about depth interpretation since much of it comes from the applied depth weighting.

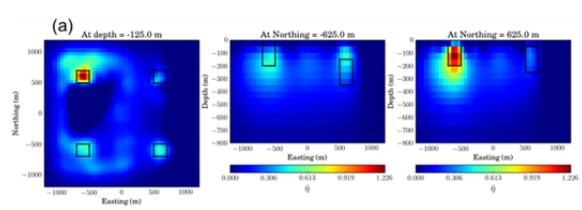

GEM Chengdu 2015: International Workshop on Gravity, Electrical & Magnetic Methods and Their Applications
Chengdu, China. April 19-22, 2015.

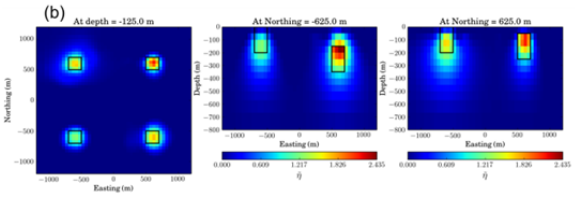

Figure 5: Plan and sections views of estimated pseudo-chargeability model at 1.25 ms. (a) pseudo-chargeability model by inverting true d^{IP} data. (b) pseudo-chargeability model by inverting observed d^{IP} data.

Inverting multiple time channels

We have concentrated upon the early time channel 1.25ms because it presents a challenge to many of our assumptions. We were able to show that chargeable bodies for a coincident loop system could be identified even when the observations are positive. Later times are less affected by EM coupling and chargeable regions are more easily identified and the data inverted.

Equation (11) shows that pseudo-chargeability recovered at any time, t, depends upon how the time history of the electric field at that location. In computing sensitivities, and polarization currents, we have normalized our system by the maximum strength and direction of the electric field at each point in space and at each time. The recovered pseudo-chargeability may therefore be expected to behave somewhat like the intrinsic chargeability obtained in EIP experiments. To test this we invert multiple time channels individually. The pseudo-chargeability for a pixel at the center of each anomaly is provided in Table I. We note that the recovered pseudo-chargeabilities change their values in accordance with the true ones, so the relative strengths of polarization are recovered.

Table 1: Comparison of true and recovered instrinsic IP parameters at four blocks.

Division	True ($[(1-\eta)\,\tau]^{-1}$)	Estimated ($[(1-\eta)\,\tau]^{-1}$)
A1 (η=0.5, τ=0.005)	400	255
A2 (η=0.5, τ=0.005)	400	256
A3 (η=0.4, τ=0.005)	333	241
A4 (η=0.8, τ=0.005)	1000	418

Field data examples

The above process has been applied to two field examples. The first is from airborne ATEM data at Mt. Milligan, a porphyry system in British Columbia. The second is from an airborne survey over a diamondiferous kimberlite in the Great Slave province in Canada.

Conclusions

We have provided an explicit workflow for extracting chargeability information from time domain inductive sources. The work has focussed on airborne data with a moving coincident loop but it is applicable to ground surveys with multiple receivers for each transmitter. A major requirement is the estimation of a background conductivity since this is used to evaluate the d^{IP} data and to compute the sensitivity matrix needed for the inversion. Further work and verification of our procedure is required but both synthetic and field examples show promising results.

References

Kang, S. and Oldenburg D. W, 2015, Recovering IP information in airborne-time domain electromagnetic data: 24th meeting ASEG-PESA, Perth, Expanded Abstracts.

Cole, K. S. and Cole, R. H., 1941, Dispersion and absorption in dielectrics i. alternating current characteristics: The Journal of Chemical Physics, 9(4), 1941.

Marchant, D., Haber E., and Oldenburg, D. W., 2015, Three-dimensional modeling of IP effects in time-domain electromagnetic data, Geophysics, 79(6), E303-E314.

Oldenburg, D. W. and Li., Y., 1994, Inversion of induced polarization data: Geophysics, 59(9), 1327–1341.

Routh, P. S. and Oldenburg D. W., 2001, Electromagnetic coupling in frequency-domain induced polarization data: a method for removal: Geophysical Journal International, 145(1):59–76, 2001

Seigel, H., Mathematical formulation and type curves for induced polarization: Geophysics, 24(3):547–565, 1959.

Smith, R., Walker, P., Polzer, B., and West, G. F., 1988, The time-domain electromagnetic response of polarizable bodies: an approximate convolution algorithm: Geophysical Prospecting, 36, 772–785.

Weidelt, P., 1982, Response characteristics of coincident loop transient electromagnetic systems: Geophysics, 47, 1325–1330.

Yang, D., Oldenburg, D. W., and Haber, E., 2014, 3-d inversion of airborne electromagnetic data parallelized and accelerated by local mesh and adaptive soundings: Geophysical Journal International, 196, 1942–1507.

GEM Chengdu 2015: International Workshop on Gravity, Electrical & Magnetic Methods and Their Applications
Chengdu, China. April 19-22, 2015.